Mass transfer in bubble column for industrial conditions—effects of organic medium, gas and liquid flow rates and column design

H. Chaumat[a], A.M. Billet-Duquenne[a,*], F. Augier[b], C. Mathieu[b], H. Delmas[a]

[a] *Laboratoire de Génie Chimique, Z.A Basso Cambo, 5 rue Paulin Talabot, 31106 Toulouse cedex 1, France*
[b] *Rhodia, Centre de Recherches de Lyon, 85 av. des Frères Perret, B.P 62, 69192 St. Fons cedex, France*

Abstract

Most of available gas–liquid mass transfer data in bubble column have been obtained in aqueous media and in liquid batch conditions, contrary to industrial chemical reactor conditions. This work provides new data more relevant for industrial conditions, including comparison of water and organic media, effects of large liquid and gas velocities, perforated plates and sparger hole diameter.

The usual dynamic O_2 methods for mass transfer investigation were not convenient in this work (cyclohexane, liquid circulation). Steady-state mass transfer of CO_2 in an absorption–desorption loop has been quantified by IR spectrometry. Using a simple RTD characterization, mass transfer efficiency and k_La have been calculated in a wide range of experimental conditions.

Due to large column height and gas velocity, mass transfer efficiency is high, ranging between 40% and 90%. k_La values stand between 0.015 and 0.050 s^{-1} and depend mainly on superficial gas velocity. No significant effects of column design and media have been shown. At last, using both global and local hydrodynamics data, mass transfer connection with hydrodynamics has been investigated through k_La/ε_G and k_La/a.

Keywords: Bubble column; Measurement method; Mass transfer; Multiphase flow; Hydrodynamics; Residence time distribution

1. Introduction

In gas–liquid processes, the mass transfer volumetric coefficient k_La is the key parameter to estimate reactor performance. Many experimental works and correlations are available on this topic (Akita and Yoshida, 1974; Hikita et al., 1981; Shah et al., 1982; Ozturk et al., 1987; Sotelo et al., 1994; Zhao et al., 1994; Kang and Cho, 1999; Jordan and Schumpe, 2001) but most of them concern only batch aqueous liquids while many industrial conditions involve organic liquids at significant liquid velocities.

Generally, mass transfer data are derived from transient oxygen concentration measurements in dynamic absorption or desorption of oxygen in the reactor (Akita and Yoshida, 1974; Ozturk et al., 1987; Deckwer, 1992; Letzel et al., 1999). However, this technique is much less recommended with flowing liquids and very fast transfer due to much more complex data treatment including slow probe dynamics. More importantly, when volatile organic liquids are involved, drastic security requirements prohibit oxygen as the transferred gas in laboratories.

The first objective of this study is the elaboration of a specific mass transfer measurement method, dedicated to contactors that run with solvents and with continuous liquid flow. The application of this method allows the estimation of the influence of liquid medium (organic or aqueous), gas and liquid flow rates, sparger type, and internals on the volumetric mass transfer coefficient. At last, coupled with hydrodynamics data, the connection between hydrodynamics and mass transfer phenomena will be considered.

* Corresponding author. Tel.: +33 5 34 61 52 56; fax: +33 5 34 61 52 53.
E-mail addresses: Helene.Chaumat@ensiacet.fr (H. Chaumat), AnneMarie.Billet@ensiacet.fr (A.M. Billet-Duquenne).

2. Pilot plant

Experiments are performed in a semi-industrial pilot plant composed by a bubble column reactor ($D_C = 0.2$ m; $H_C = 1.6$ m aerated liquid) and a gas–liquid separator (cf. Fig. 1). The liquid is circulated by a pump. Two toroidal gas spargers of 0.8% free area, pierced with different hole size (respectively, $d_0 = 0.001$ and 0.0005 m), have been successively used. The effect of four perforated partition plates (14 holes of 30 mm), introduced with the sparger with 0.001 m holes as mentioned in Fig. 1, has also been tested.

Liquid phase is either organic (cyclohexane) or aqueous (tap water) (properties reported in Table 1). When organic liquid is used, a cryogenic apparatus is linked to the gas outlet so that organic vapor is fully recovered. For safety reasons, the gas introduced in the bubble column is N_2, gas inert with the studied liquids (the gas properties are detailed in Table 2).

Large ranges of gas superficial velocity (up to 0.14 m/s) and superficial liquid velocity (up to 0.08 m/s) have been investigated. All experiments are run at atmospheric pressure and around 20 °C.

Within the bubble column, global gas hold-up has been measured with a differential pressure transducer; it includes the main part of the column, except the part under the sparger and the disengagement zone (cf. Fig. 1). In order to obtain a liquid phase model, residence time distribution (RTD) has been performed by usual tracer analysis. Data of mean Sauter diameter, estimated with an optic double probe, are also available; the values used in this study are measured at 0.65 m of the bottom.

Table 1
Liquid properties

Liquid	Formula	Molar weight (g/mol)	Density (water = 1)	Viscosity (mPa s)	Superficial tension (mN/m)
Cyclohexane	C_6H_{12}	84	0.78	0.894	24.65
Water	H_2O	18	1	0.890	71.99

Table 2
Gas properties

Gas	Molar weight (g/mol)	Density (air = 1)
N_2	24	0.97
CO_2	44	1.54

3. Mass transfer measurement method

In order to investigate mass transfer in a bubble column operated with liquid flow, steady-state mass transfer conditions are often preferred to avoid uncertainty due to slow probe dynamics (Delmas et al., 1988; Syaiful et al., 1995). For steady-state operation the liquid has to successively absorp and desorb in a loop.

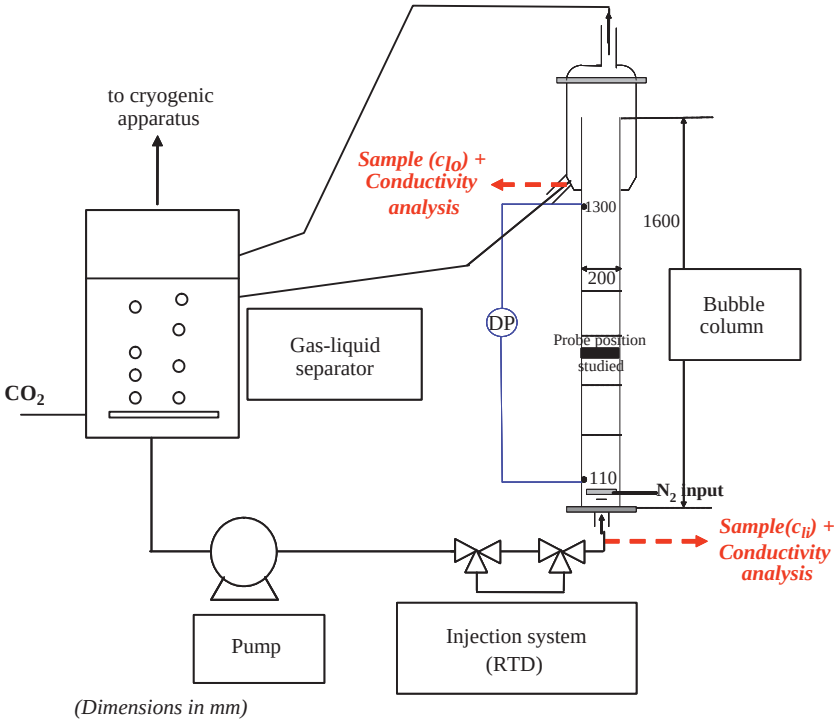

Fig. 1. Pilot plant for mass transfer measurement.

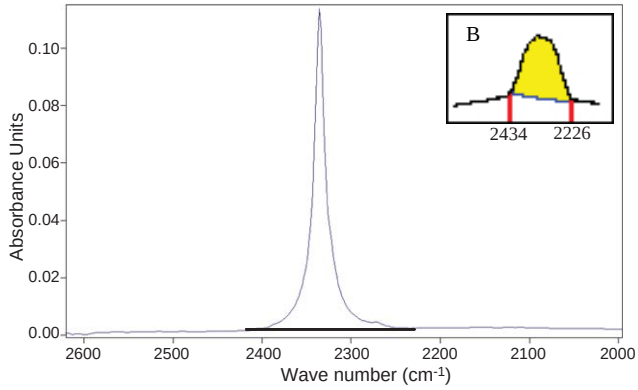

Fig. 2. Example of dissolved CO_2 peak (cyclohexane).

In this pilot plant, the gas–liquid separator is used to absorb a gas and its desorption through the bubble column fed with nitrogen is quantified. The selected gas is carbon dioxide (gas properties detailed in Table 2), because it is moderately soluble both in water (about 33 mol/m^3 (Lide, 1997)) and in cyclohexane (about 55 mol/m^3 (Wilhelm and Battino, 1973)), inert with cyclohexane (avoiding safety problems) and analytically quantifiable. CO_2 dissolved concentration is measured thanks to an IR spectrometer, equipped with a circulation attenuated total reflexion (ATR) accessory. The dissolved CO_2 concentration is deduced, after calibration, from CO_2 peak area located between 2226 and 2434 cm^{-1} (cf. Fig. 2).

In the bubble column, input (c_{Li}) and output (c_{Lo}) dissolved CO_2 concentrations are measured, as shown in Fig. 1, following a strict withdrawal procedure. Those positions have been chosen on input and output pipes, in order to limit the radial gradient of CO_2 and to avoid bubble presence, which could affect the measurements validity.

Those concentrations lead easily to mass transfer efficiency, defined as the ratio of desorbed CO_2 in the column ($c_{Li} - c_{Lo}$) in comparison with input amount of CO_2 (c_{Li}):

$$\text{efficiency} = \frac{c_{Li} - c_{L0}}{c_{Li}}. \tag{1}$$

To evaluate a volumetric mass transfer coefficient, k_La, mass balance equations in both phases have to be solved. As a first approximation, a simple model for gas and liquid flows through the column is convenient. The liquid flow model is derived from experimental RTD measured in aqueous medium by injecting a KOH pulse at the bottom of the column (about 10 g); the conductivity evolutions is then recorded at column input and output (to have representative results, the input and output positions are the same as for transfer measurements, cf. Fig. 1). Once mean residence time (τ) and RTD variance (σ) are calculated from input and output data, a number of equivalent perfectly mixed reactors continuous stirred tank reactor (CSTR), N, is associated at each experimental condition by

$$\frac{\sigma^2}{\tau^2} = \frac{1}{N}. \tag{2}$$

As tracer analysis was not available for the gas phase, the CO_2 concentration is assumed uniform in a CSTR. This concentration can be considered equal to the CSTR outlet concentration, which corresponds to the same flow model as for the liquid phase (N CSTR in series). But the gas flow is usually less dispersed than the liquid flow, even supposed plug flow in many works, so the gas concentration would rather be calculated as the average between inlet and outlet values for each CSTR. Both gas flow models have been checked in order to estimate the influence of the gas flow models on k_La results.

For k_La estimation, Henry's constants are also needed. The large scattering of Henry's constant for CO_2–water in literature suggests a strong effect of liquid purity and or pH. As tap water and crude cyclohexane are used in this work, Henry's constants have been determined experimentally by varying pressure in a stirred autoclave (at 20 °C, pressure between 1 and 8 bar), rather than taken from literature. Henry's constants are respectively, 1838 Pa m^3/mol for cyclohexane and 3105 Pa m^3/mol for water.

4. Global hydrodynamics data

First of all, to better know the investigated flows, global hydrodynamics of both phases are briefly described.

4.1. Gas phase

Gas phase hydrodynamics is characterized through gas hold-up evolution with superficial gas velocity. As shown by Fig. 3, such evolutions are quite usual: gas hold-up grows with gas flow rates and reaches about 25% at 0.12 m/s. However, the classical homogeneous regime is not observable, except for cyclohexane at $u_L = 0.04$ m/s with $d_0 = 0.005$ m. Fig. 3 confirms the well-known sparger effect: a decrease in sparger hole diameter leads to a slight increase on gas hold-up at low gas velocity while it has no effect when heterogeneous hydrodynamic regime is established ($u_G > 0.07$ m/s for $u_L = 0.04$ m/s with cyclohexane). Fig. 4 exhibits the less known effect of liquid velocity influence: global gas hold-up decreases as superficial liquid velocity rises. As for the media influence, only a weak gas hold-up diminution is observed when water is used instead of cyclohexane despite a much larger superficial tension (Fig. 4). At last, the weak effect of perforated partition plates on gas hold-up is pointed out on Fig. 3.

4.2. Liquid phase

Liquid phase hydrodynamics is characterized through equivalent CSTR numbers, derived from RTD experiments,

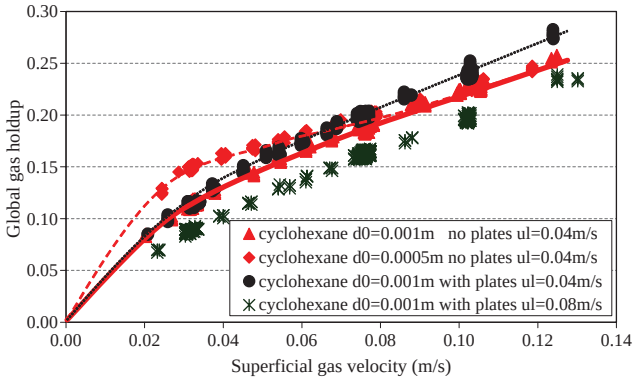

Fig. 3. Effect of sparger holes diameter and perforated plates on gas holdup evolution with superficial gas velocity (cyclohexane).

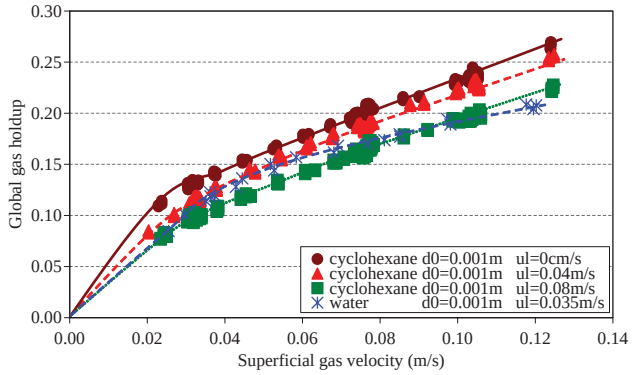

Fig. 4. Effect of superficial liquid velocity and liquid medium on gas hold-up evolution with superficial gas velocity.

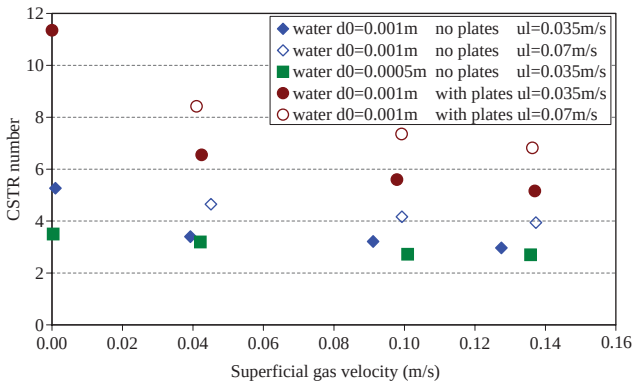

Fig. 5. Characterization of liquid phase hydrodynamics (in water).

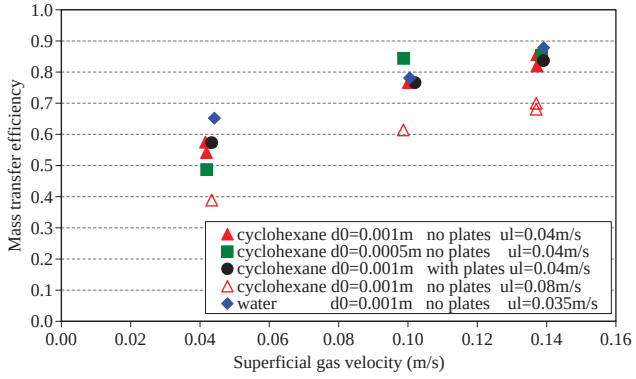

Fig. 6. Evolution of mass transfer efficiency with superficial gas velocity.

as previously mentioned. As the selected RTD method is based on inlet and outlet conductivity measurements, the only available data concern water. Nevertheless, regarding the abovementioned slight difference between gas hold-up in water and in cyclohexane, the CSTR numbers have been supposed equal for the two liquids and depending only on gas and liquid flow rates and on column design.

A slight diminution in CSTR number, i.e., a slight increase in liquid mixing, is observed when the superficial gas velocity increases (cf. Fig. 5), effect which nevertheless remains weaker than expected. Superficial liquid velocity rise induces a clear increase in CSTR number (cf. Fig. 5). As for the design effects (cf. Fig. 5): sparger hole diameter effect is negligible, whereas the introduction of partition plates clearly deals to an increase of CSTR number, the backmixing being hindered.

5. Mass transfer

Mass transfer results are divided into three parts: first mass transfer efficiency and volumetric mass transfer coefficient will be successively presented, then the relationship between hydrodynamics and transfer will be questioned.

5.1. Mass transfer efficiency

The mass transfer efficiency is the easiest mass transfer parameter to calculate, as it does not depend on flows models. Its repeatability has been found within 6%.

The effects of studied parameters on mass transfer efficiency are presented in Fig. 6. As expected, mass transfer efficiency increases with superficial gas velocity: the more gas there is, the more turbulence and mainly the more interfacial area there are. The negative effect of increasing liquid velocity is also easy to understand as it reduces the liquid residence time and to a less extent the gas hold-up.

Concerning the liquid medium, although gas hold-up is slightly greater in cyclohexane than in water, no difference is observed in mass transfer efficiency. Design effects are somewhat surprising too: neither the sparger hole diameter, nor the partition plates significantly alter the mass transfer efficiency. However these results are not contradictory to hydrodynamics, showing only little gas hold-up variations. As a conclusion, mass transfer efficiency is less sensitive to liquid medium and to column design than the gas hold-up.

Mass transfer efficiency exhibits first tendencies, allowing some comparisons at given liquid and gas flow rates, but this overall parameter does not provide an absolute

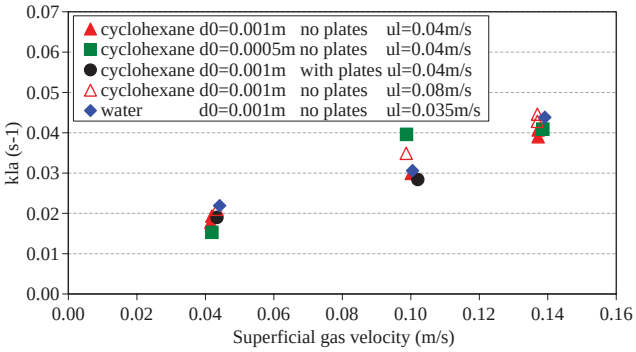

Fig. 7. Evolution of volumetric mass transfer coefficient with superficial gas velocity.

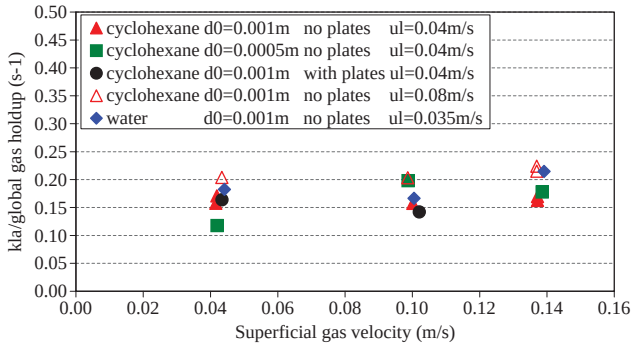

Fig. 8. Evolution of k_La/ε_G ratio with experimental conditions.

qualification of the mass transfer ability in the investigated reactor, particularly as it depends on the column height used. The useful parameter for a reactor mass transfer characterization and for predictive modelling is the volumetric mass transfer coefficient k_La.

5.2. Volumetric mass transfer coefficient, k_La

k_La values are optimized from inlet and outlet CO_2 concentrations in the liquid phase, according to the mass balance on each CSTR.

For i CSTR:

$$c_L(i)Q_L + c_G(i)Q_G(i) = c_L(i+1)Q_L + c_G(i+1)Q_G(i+1), \quad (3)$$

$$c_L(i)Q_L = c_L(i+1)Q_L - k_La V_{\mathrm{CSTR}}(c^*(i) - c_L(i)) \quad (4)$$

with

$$c^*(i) = \frac{((c_G(i) + c_G(i+1))/2)RT}{He} \quad (5)$$

or,

$$c^*(i) = \frac{c_G(i)RT}{He} \quad (5')$$

$$Q_G(i) = \frac{P_i Q_{Gi} + (c_{Li} - c_L(i))Q_L RT}{P(i)}, \quad (6)$$

$$P(i) = P_{\mathrm{atm}} + \rho_L(1-\varepsilon_G)g(H_C - z(i)), \quad (7)$$

$$z(i) = i H_{\mathrm{CSTR}} = i\,\frac{H_C}{N}. \quad (8)$$

Whatever the assumption for the gas flow (Eq. (5) or Eq. (5′)), the deviation in k_La between two repeated experiments is larger for k_La than for the efficiency, but stands lower than 10% as shown in Fig. 7. Eq. (5) leads to smaller values of k_La than Eq. (5′), the relative difference ranging from 4% to 30%. According to literature the actual gas flow should be closer to plug flow than to perfectly mixed on each CSTR; then the following results have been derived using with Eq. (5).

Fig. 7 sums up the main tendencies. k_La increases with superficial gas velocity, like mass transfer efficiency. Design effects are also similar to those obtained previously in mass transfer efficiency: no effect of sparger hole diameter and of partition plates introduction is observed. Mass transfer coefficients are equivalent for water and cyclohexane in same conditions, as observed on efficiency, but are slightly increasing with superficial liquid velocity.

5.3. Relation between hydrodynamics and mass transfer

The comparison between hydrodynamics and mass transfer results is now considered. For this purpose, k_La is successively related to the global gas hold-up, ε_G, and to the interfacial area, a.

5.3.1. k_La/ε_G

In the literature, the mass transfer coefficient is often directly correlated to global gas hold-up instead of operating parameters. For example, some correlations predict k_La from global gas hold-up data to the power of 1–1.18, with no dependence on superficial gas velocity (Akita and Yoshida, 1974; Shah et al., 1982; Elgozali et al., 2002). As a first approximation, k_La would be proportional to ε_G : $k_La = \alpha\varepsilon_G$, where α depends on design column and liquid medium. According to Letzel et al. (1999) and Vandu and Krishna (2004), $\alpha = 0.5\,\mathrm{s}^{-1}$ and this universal relationship characterizes the heterogeneous hydrodynamic regime. Such a relationship, if largely validated, would highly simplify k_La determination. No specific k_La measurement would be required as the global gas hold-up is much easier to get.

In this work, k_La/ε_G, plotted as a function of superficial gas velocity in Fig. 8, ranges between 0.1 and $0.3\,\mathrm{s}^{-1}$, at much lower values than proposed above. In addition, this ratio is not a constant even in heterogeneous regime: it increases with superficial liquid velocity. As a matter of fact, when superficial liquid velocity rises, the global gas hold-up decreases more than k_La. However, liquid medium has no significant effect. At last, there is no clear design influence on k_La/ε_G, as both hydrodynamics and mass transfer are not very altered by these modifications (sparger hole

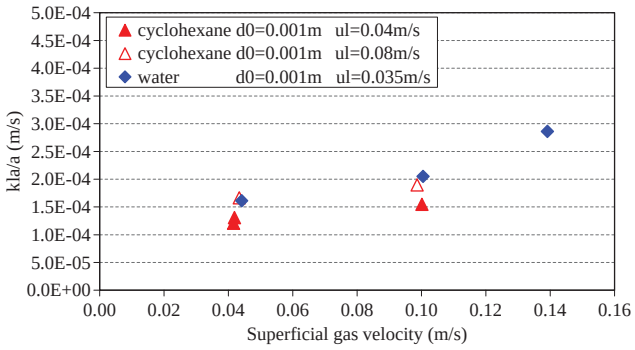

Fig. 9. Evolution of k_La/a ratio with experimental conditions.

diameter or partition plates introduction). To conclude, the connection between ε_G and k_La appears more complex than the oversimplified $k_La = \alpha\varepsilon_G$.

5.3.2. k_La/a

Thanks to double optic probe measurement, local interfacial area measurements are available and the ratio k_La/a can be estimated. In principle, k_La/a calculation leads to k_L estimation. However, it is not exactly as simple here, because k_La and a are not determined at the same scale: k_La is a global mass transfer parameter based on inlet and outlet concentrations while the interfacial area a is a local estimation by a double optic probe. Results of local interfacial area are presented elsewhere (Chaumat, 2004). Briefly, for a given set of experimental conditions, the axial and radial variations of local interfacial area are significant, while the mean Sauter diameter deduced from same recordings is nearly uniform. This means that these local variations of interfacial area are mainly due to local variations of the gas hold-up. In order to use a more global interfacial area, a is deduced from the average Sauter mean diameter on the whole column and the global gas hold-up by

$$a = \frac{6\varepsilon_G}{d_{SM}}. \tag{9}$$

Note that d_{SM} is smaller in cyclohexane (d_{SM} from 0.0035 to 0.0063 m for the present cases) than in water (d_{SM} from 0.0039 to 0.0081 m).

The runs with perforated plates have not been presented here, because in this case large axial variations have been observed both for a and d_{SM}, that hinders global interfacial area determination.

The apparent mass transfer coefficient k_La/a increases with superficial gas velocity contrary to Higbie's theory, suggesting a positive effect of bubble induced turbulence on the mass transfer coefficient. From Fig. 9, k_La/a values are ranging between 1×10^{-4} and 4×10^{-4} m/s. For comparison, k_L values calculated from different approaches are summarized in Table 3. The best fit is found for the correlations of Akita and Yoshida (1974) and of Schügerl et al. (1978). Data issued from water are higher than from cyclohexane; this trend is in agreement with most of the tested correlations, except Akita and Yoshida (1974) (Table 3). Increasing liquid superficial velocity seems to increase k_La/a, as expected, due to smaller interfacial area (Chaumat, 2004).

Table 3
k_L calculation with different approaches (cf. Bird et al., 1960; Shah et al., 1982) ($d_{SM} = 0.005$ mm)

Authors	k_L	
	Cyclohexane	Water
Higbie ($u_S = 0.25$ m/s)	3.50×10^{-4}	
(Calderbank and Moo-Young, 1961)	3.85×10^{-6}	4.01×10^{-6}
(Hughmark, 1967) ($u_G = 0.10$ m/s)	7.54×10^{-4}	8.00×10^{-4}
Akita and Yoshida (1974)	3.14×10^{-4}	2.30×10^{-4}
(Gestrich et al., 1976) ($u_G = 0.10$ m/s)	1.05×10^{-2}	1.96×10^{-2}
Schügerl et al. (1978)	1.34×10^{-4}	1.43×10^{-4}

6. Conclusions

An experimental mass transfer measurement method, working in steady-state conditions, has been successfully carried out in typical industrial conditions (high gas and liquid flow rates, solvents); however, to get a better precision on derived k_La values, it would be convenient to analyze the gas flow with the RTD technique.

Main effects of gas and liquid flow rates, column design (sparger hole diameter and perforated plates) and liquid medium on the equivalent CSTR number, mass transfer efficiency and volumetric mass transfer coefficient have been determined; they are summarized in Table 4. Surprisingly the partition plates introduction and thee liquid medium have no significant effect on the volumetric mass transfer coefficient; only superficial gas velocity has a clear influence. Coupled with hydrodynamics, those experiments show the complex relationship between k_La and ε_G : k_La/ε_G is not strictly constant as this ratio depends on u_L and on the liquid medium. Nevertheless the relation $k_La = \varepsilon_G/6$ would provide a correct order of magnitude in the large range of operation conditions tested here.

Table 4
Summary of the main effects observed on CSTR number, volumetric mass transfer efficiency and k_La

	CSTR number	Efficiency	k_La
Superficial gas velocity	⇘	⇖	⇖
Superficial liquid velocity	⇖	⇘	⇖ (slightly)
Sparger hole diameter	⇨	⇨	⇨
Partition plates presence	⇖	⇨	⇨
Liquid medium		⇨	⇨

At last, thanks to optic probe interfacial area measurements, a rough estimation of a global liquid side mass transfer coefficient k_L has been obtained as k_La/a; this parameter increases with superficial gas velocity suggesting some effects of bubble-induced turbulence.

Notation

a	interfacial area, m^2/m^3
c_G	CO_2 concentration in gas phase, mol/m^3
c_L	CO_2 concentration in liquid phase, mol/m^3
c_{Li}	input dissolved CO_2 concentration, mol/m^3
c_{Lo}	output dissolved CO_2 concentration, mol/m^3
$c*$	dissolved CO_2 concentration at saturation, mol/m^3
d_0	sparger hole diameter, m
d_{SM}	sauter mean diameter, m
D_C	column diameter, m
g	gravity acceleration, m^2/s
H_C	column height, m
H_{CSTR}	CSTR height, m
He	Henry's constant, $Pa\,m^3/mol$
i	CSTR number studied, dimensionless
k_L	liquid side mass transfer coefficient, m/s
k_La	volumetric mass transfer coefficient, s^{-1}
N	CSTR number, dimensionless
P	pressure, Pa
P_{atm}	atmospheric pressure, Pa
P_i	input pressure, Pa
Q_G	gas flow rate, m^3/s
Q_{Gi}	input gas flow rate, m^3/s
Q_L	liquid flow rate, m^3/s
R	perfect gas constant, $Pa\,m^3\,mol^{-1}\,K^{-1}$
T	temperature, K
u_L	superficial liquid velocity, m/s
u_G	superficial gas velocity, m/s
u_S	slip velocity, m/s
V_{CSTR}	CSTR volume, m^3
z	height, m

Greek letters

α	proportionality coefficient between k_La and ε_G, s^{-1}
ε_G	global gas hold-up, dimensionless
ρ_L	liquid density, kg/m^3
σ	RTD variance, s
τ	mean residence time, s

References

Akita, K., Yoshida, F., 1974. Bubble size, interfacial area, and liquid phase mass transfer coefficients in bubble columns. Industrial Engineering Chemical Process Design and Development 12, 84–91.

Bird, R.B., Stewart, W.E., Lightfoot, E.N., 1960. Transport Phenomena. Wiley, New York, p. 541.

Calderbank, P.H., Moo-Young, M.B., 1961. The continuous phase heat and mass transfer properties of dispersion. Chemical Engineering Science 16, 39–54.

Chaumat, H., 2004. Hydrodynamique locale et globale d'une colonne à bulles en conditions industrielles. Ph.D. thesis, INPT, Toulouse, France.

Deckwer, W.D., 1992. Bubble Column Reactors. Wiley, New York.

Delmas, H., Huang, H., Mawlana, A., Riba, J.P., Wang, Y.B., 1988. Deux approches du transfert de matiére gaz–liquide en fluidisation á trois phases. Entropie 143–144, 33–48.

Gestrich, W., Eisenwein, H., Krauss, W., 1976. Der flüssigkeitsseitige stoffübergangskoeffiizient in blasenschichten. Chemie Ingenieur Technik 48, 399–407.

Hughmark, G.A., 1967. Holdup and mass transfer in bubble columns. Industrial Engineering Chemical Process Design and Development 6, 218–220.

Elgozali, A., Linek, V., Fiavola, M., Wein, O., Zahradnik, J., 2002. Influence of viscosity and surface tension performance of gas–liquid contactors with ejector type gas distributor. Chemical Engineering Science 57, 2987–2994.

Hikita, H., Asai, S., Tanigawa, K., Kitao, M., 1981. The volumetric liquid-phase mass transfer coefficient in bubble column. Chemical Engineering Journal 22, 61–69.

Jordan, U., Schumpe, A., 2001. The gas density effect on mass transfer in bubble columns with organic liquids. Chemical Engineering Science 56, 6267–6272.

Kang, Y., Cho, Y.T.J., 1999. Diagnosis of bubble distribution and mass transfer in pressurized bubble columns with viscous liquid medium. Chemical Engineering Science 54, 4887–4893.

Letzel, M.H., Schouten, J.C., Krishna, R., van den Bleek, C.M., 1999. Gas hold-up and mass transfer in bubble column reactors operated at elevated pressure. Chemical Engineering Science 54, 2237–2246.

Lide, R.D., 1997. Handbook of Chemistry and Physics. 78th ed. 1997–1998. CRC Press, Boca Raton, FL.

Ozturk, S.S., Schumpe, A., Deckwer, W.D., 1987. Organic liquids in a bubble column: hold-ups and mass transfer coefficients. A.I.Ch.E. Journal 33, 1473–1480.

Shah, Y.T., Kelkar, B.G., Godbole, S.P., 1982. Design parameters estimations for bubble column reactors. A.I.Ch.E. Journal 28, 353–378.

Sotelo, J.L, Benitez, F.J., Beltran-Heridia, J., Rodriguez, C., 1994. Gas hold-up and mass transfer coefficients in bubble columns. 1. Porous glass–plate diffusers. International Chemical Engineering 34, 82–90.

Syaiful, Wilhelm, A.M., Svendsen, H., Delmas, H., 1995. Analysis of three upward cocurrent gas–liquid–(solid) contactors: gas hold-up, axial dispersions, gas–liquid mass transfer. Transactions of the Institution of Chemical Engineering 73 (Part A), 643–648.

Vandu, C.O., Krishna, R., 2004. Influence of scale on the volumetric mass transfer coefficients in bubble columns. Chemical Engineering and Processing 43, 575–579.

Wilhelm, E., Battino, R., 1973. Thermodynamics functions of the solubilities of gases in liquids at 25 °C. Chemical Reviews 73, 111–120.

Zhao, M., Niranjan, K., Davidson, J.F., 1994. Mass transfer to viscous liquids in bubble columns and air-lift reactors: influence of baffles. Chemical Engineering Science 49, 2359–2369.